

# Towards the trans-GZK era from giant EAS arrays to satellite experiments

Jean-Noël Capdevielle<sup>1</sup>

**Abstract**—The present data on giant air showers supports the existence of the GZK cut off, but some problems concerning the mass composition remain. Simulations have been carried out to understand the discrepancy between AUGER, HIRES and AGASA at ultra high energy. Above the GZK cutoff, we explore also the interest of experiments borne on satellites such as the JEM-EUSO project on the ISS taking the advantage of collection areas near 1 million  $km^2$ .

## I. INTRODUCTION

The number of showers collected in AUGER as well as in HIRES above 70 EeV falls rapidly, suggesting a behaviour in agreement with GZK cut off. After considering some circumstances reducing the primary energy of the larger number of events previously obtained in AGASA, we obtain a tendency to a tolerable agreement among giant and hybrid fluorescence arrays.

A few events remain above 100 EeV and the question arises if those ultra high energy events characterized by a maximum depth at very high altitude have a common origin with the events of lower energy or if those showers start with a different type of interaction. To compensate the statistical deficit, we examine the interest of satellite borne experiments detecting the fluorescence of the showers from the ISS. The feasibility of  $\gamma$  Ray Astronomy at ultra high energy together with Hadron Astronomy is considered for the JEM-EUSO project.

## II. THE CASE OF GIANT SURFACE ARRAYS AND HYBRID EXTENSIONS

Extensive simulations with CORSIKA code [5] have been performed for  $\gamma$ 's, protons and iron nuclei as primary particles for 6 energies and in most cases for 8 different zenith angles. The observation level corresponded mainly to the Auger experiment. In each combination of primary particle, energy and zenith angle, 40 EAS have been simulated. Previous simulations at different levels such as AGASA, Haverah Park and Yakutsk [7] have also been involved in the present approach.

### A. The energy overestimation in the treatment of inclined showers

The major part of the data concerns individual inclined EAS where the basic characteristics are first collected and sorted during the earliest analysis: zenith angle from timing on different detectors, axis position from adjustment on different densities with relations similar to 2. The most probable density at the distance selected for the estimator (600 m for

AGASA, 1000 m for AUGER) is derived from the best analytic distribution fitted to the densities on the detectors. Density  $\rho_{600}(\theta)$  is used to determine  $S_{600}(\theta)$  which is in turn converted to the value of the estimator for shower generated by the same primary Cosmic Ray particle at vertical incidence. This conversion inferred by fitting the attenuation of  $S_{600}$  [14] is represented by:

$$S_{600}(\theta) = S_{600}(0) \times \exp\left(-\frac{t_0}{\Lambda_1}(\sec(\theta) - 1) - \frac{t_0}{\Lambda_2}(\sec(\theta) - 1)^2\right) \quad (1)$$

The values  $\Lambda_1 = 500 \text{ gcm}^{-2}$  and  $\Lambda_2 = 594_{-130}^{+268} \text{ gcm}^{-2}$  were describing the data on showers with  $\theta \leq 60^\circ$ .

The primary energy  $E_0$  (in eV) is recovered for the most recent data with the conversion of AGASA [12]:

$$E_0 = 1.96 \cdot 10^{19} \left(\frac{S_{600}(0^\circ)}{100}\right)^{1.02} \quad (2)$$

The simulations at ultra high energy contradict the classical absorption behaviour of relation 1 (the lowest line in Fig. 1): the density increases progressively in function of the primary energy versus  $\sec(\theta)$  reaching a maximum between  $10^\circ - 20^\circ$  and then decreases with zenith angle for primary protons ( $E_0 = 10^9, 5 \cdot 10^9, 10^{10}, 5 \cdot 10^{10}, 10^{11} \text{ GeV}$ ). The dependence shown in Fig. 1 is a general consequence of the electromagnetic cascade theory. In contrast with the description of the attenuation by relations similar to relation 1, i.e. monotonously decreasing functions, the measurements of attenuation by the method of constant intensity cuts have to be performed with functions able to rise versus  $\sec(\theta)$ , reach a maximum and finally decrease at large  $\theta$  for primary energies exceeding  $5 \cdot 10^{18} \text{ eV}$ . The distorted gaussian function 3 is introduced hereafter to fulfil those properties.

A similar increase of the estimator density appears in the calculations performed with AIRES [16], plotted versus the distance between the experimental plane and the maximum depth (the upper dashed curve corresponds here to the extremal circumstance where the maximum depth coincides with the level of AGASA). The behaviour shown in fig.1 (solid curves from our calculation) in the case of AUGER corresponds to a maximum depth of the longitudinal development at about one electron radiation length (for  $E_0 = 10^{11} \text{ GeV}$ ) above the experimental array (a similar situation in AGASA would be obtained with a model of modest multiplicity such as HDPM or DPMJET). For a model with large multiplicity, such as

<sup>1</sup>APC Astroparticules et Cosmologie, Univ. Paris-Diderot, 10 rue Alice Domont et Leonie Duquet, 75205 Paris, France, capdev@apc.univ-paris7.fr

TABLE I

TABLE OF COEFFICIENTS  $A$ ,  $\langle l \rangle$ ,  $\sigma$ ,  $s$  AND  $k$  VERSUS ENERGY FOR AUGER

$E_0$ (eV)	$A$	$\langle l \rangle$	$\sigma$	$s$	$k$
$10^{18}$	1.0	1.0	0.37	0.020	$0.18 \cdot 10^{-5}$
$5 \cdot 10^{18}$	1.01	1.03	0.38	0.0019	$0.24 \cdot 10^{-6}$
$10^{19}$	1.03	1.09	0.34	0.10	$0.3 \cdot 10^{-4}$
$5 \cdot 10^{19}$	1.06	1.15	0.34	0.16	$0.24 \cdot 10^{-5}$
$10^{20}$	1.1	1.16	0.34	0.083	$0.14 \cdot 10^{-5}$

QGSJETII or Sybill2.1, the same maximum is near 3 radiation lengths above AGASA and the total discrepancy is slightly reduced at  $920 \text{ gcm}^{-2}$  for AGASA.

The contrast between those models characterized by higher

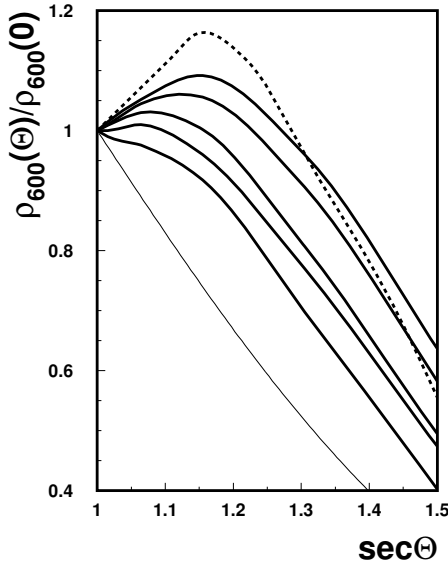


Fig. 1. Dependence  $\frac{\rho_{600}(\theta)}{\rho_{600}(0)}$  versus  $\sec(\theta)$  for protons with  $E_0 = 10^9, 5 \cdot 10^9, 10^{10}, 5 \cdot 10^{10}, 10^{11}$  GeV (from bottom to top) respectively for models of low multiplicity (thick lines). The bottom curve corresponds to formula 1). The dashed line (upper curve) corresponds to the situation at Auger level following [16].

multiplicities or lower multiplicities is emphasized by the cross sections implemented respectively in the calculation of the hadronic cascades (see for example [17]).

### B. The distorted gaussian analytic description

This typical behaviour can be described analytically by the so called distorted gaussian function:

$$f(l) = A \times \exp\left(\frac{k}{8} - \frac{s\delta}{2} - \frac{1}{4}(2+k)\delta^2 + \frac{1}{6}s\delta^3 + \frac{1}{24}k\delta^4\right) \quad (3)$$

where:  $l = \sec(\theta)$ ,  $\delta = (l - \langle l \rangle) / \sigma$

Values of parameters in formula 3 are summarized in the Table I in agreement with the figure 1.

The dependences shown in Fig. 1 are a general consequence of the electromagnetic cascade theory and the discrepancy with the original "AGASA" absorption increases as the distance from AGASA level to the shower maximum decreases. In the case of iron primaries as the maximum is higher in the atmosphere than for protons, the attenuation remains less different from relation 1 (equivalent sets of parameters presented in Table I are also available [29])

### C. Difficulties in interpretation of $T_{max}$ and attenuation measurements in AUGER

We have already compared our results with the measurements of AGASA by the method of fixed intensity cuts [11] used in AGASA to determine the relation 1

The dependence of the estimator at 1000 m from the axis has also been calculated at AUGER level for the energy of  $10^{19}$  eV [18] using the QGSJET II model. We compare in Fig. 2 our results with the model QGSJET01 to those calculations together with the experimental data of AUGER [22].

We underline that here  $S$  is not the density, but the total

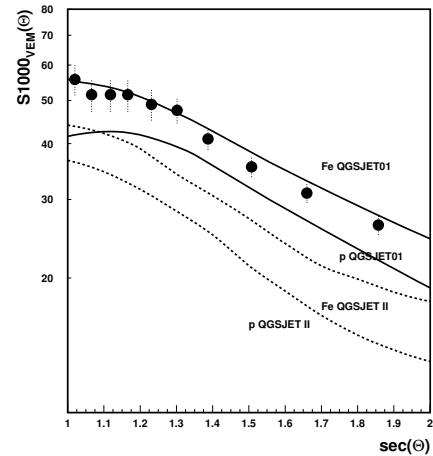


Fig. 2. Attenuation at 1000 m from axis, experimental measurements from AUGER for energy  $0.9 \cdot 10^{19}$  eV, lines from QGSJET01/GHEISHA and QGSJET II/Fluka as indicated.

number of VME's recorded on the water Cerenkov tank; our results for QGSJET01/GHEISHA for Fe and p primaries suggest that the primary component at  $10^{19}$  eV would still be very rich in heavy nuclei.

In our case, as well as for QGSJET II/FLUKA (given only for p primary) the resulting  $S$  is the sum of the em component and the muon component, both converted in VME's. The experimental data obtained by the method of constant intensity cuts in AUGER corresponds to a primary energy of  $0.9 \cdot 10^{19}$  eV : we note that QGSJET II even in case of Fe primary will not agree with the data; according to the muon component given also in [18], we estimate that for an Fe primary the total value of  $S_{1000}$  cannot reach the experimental points of Fig. 2, remaining under 50 VME's for the vertical incidence. Several features may be at the origin of the problems exhibited

by Fig. 2 concerning the difficulty to reach a tolerable agreement and the discrepancies between calculations. An earliest calculation [19] has given 47 VME's for a vertical proton of  $10^{19}$  eV for the combination QGSJET01+Fluka, 43 VME's for the combination QGSJET01+GHEISHA2002: in similar situation, we received 42 VME's as an average for 40 cascades simulated, contrasting apparently with the 37 VME's in [18] for QGSJET II + Fluka.

Considering the calculation performed with CORSIKA on maximum depth  $\langle X_{max} \rangle$  [20] very close values may be ascertained for QGSJET II and QGSJET 01 on Fig. 3, the authors pointing out near  $10^{19}$  eV an elongation rate which does not need to be explained by a very heavy primary component as required in Fig. 2.

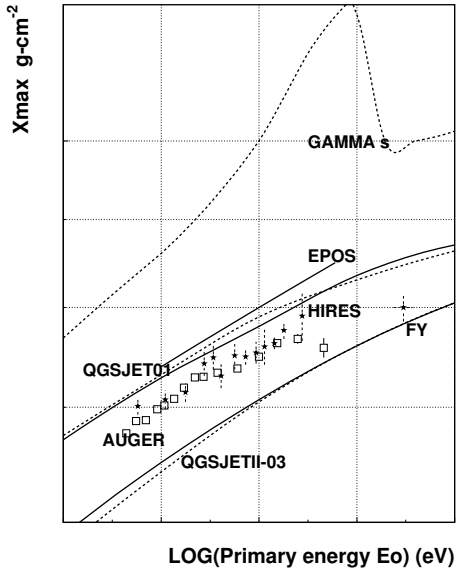


Fig. 3. Depths of shower maximum vs. primary particle energy, experimental points for Auger and HiRes, lines for QGSJET01, QGSJETII-03 as indicated and EPOS (only for protons).

The most sophisticated approach carried in [18] has taken into account the very specific responses of the water Cerenkov tanks through elaborated simulations with GEANT4. However, new considerations on the muon contribution to the signal of the water Cerenkov tank were advanced recently [23], but remain questionable about the primary energy estimation in AUGER.

Nethertheless, an excess of produced pions for QGSJET01 model was ascertained during comparisons with p-C collisions in NA49 experiment at 158 GeV/c [25]; one consequence is again an artificial excess of muons in the simulation with QGSJET01 and this circumstance supports the preference of QGSJET II for further analysis of AUGER data where the muons play an important role. Assuming the advantages of QGSJETII, the coherence between both AUGER attenuation and  $\langle X_{max} \rangle$  measurements could hardly be restored con-

sidering that the primary energy in AUGER is underestimated by at least 15% around  $10^{19}$  eV together with a mixed primary component.

#### D. Unified tendencies and convergence to GZK

We have simulated EAS with a differential primary spectrum with an ankle or with 3 spectral index like in formula 4 and compared the spectrum reconstructed with AGASA method or via our distorted gaussian function [29]. The assumed correct energy (obtained via relation 3) is then sorted in the suitable energy bin of the reconstructed histogram of the primary energy spectrum. The intensities inside the same energy bins from HBOOK are in turn compared for both histograms and the adequate reduction is applied to the points of AGASA (Fig. 4). The corrections above  $10^{20}$  eV turn to a factor of reduction by 7-10, if we consider a large number of showers in each energy bin. Our procedure is not valid for a limited number of showers and the experimental data must be sorted again in the convenient bins of energy and zenith angle event per event. Such work can be performed correctly only with the raw data of the experimentators; their revision is now in progress [12] replacing formula 1, as previously suggested by us [11] and has rejected one half of the events above 100 EeV.

Observing that some detectors of AGASA (even if the data is presented as rescaled at the level of Akeno array used for the calibration) are lying at lower altitude (around  $950 \text{ gcm}^{-2}$ ), we have repeated the procedure of Table I with a set of parameters corresponding to a distance of 3 radiation lengths between shower maximum and AGASA level. The fluctuations with an r.m.s. of 10% for  $S_{600}$  have been included (amending relation 2 by an energy reduction of 12%) and the energy reconstructed has been weighted versus the elementary solid angle. We found that after an individual treatment only 4 events might remain above  $10^{20}$  eV.

This corresponds to an overestimation of the primary energy by 17% at  $10^{18}$  eV rising to 27% at  $8 \cdot 10^{19}$  eV. Taking into account the possible underestimation of the primary energy in AUGER by 15% (section 2.3), we present the respective spectra (Fig. 5) amended as follows, after taking for AUGER the data presented in [26] and for HiRes the data of HiRes I and II, presented together with AGASA measurements in [1]:

- General increase of the primary energy by 15% in AUGER
- Correction for inclined showers similar to Table I and statistical correction in conversion 2
- HiRes I and HiRes II unchanged

A better convergence appears between the 3 spectra in Fig. 5, where we have adapted the fits used by [1] and [26] in the analytic descriptions:

$$J(E_0) = A \times \left( \frac{E_0}{E_c} \right)^{-\gamma} \quad (4)$$

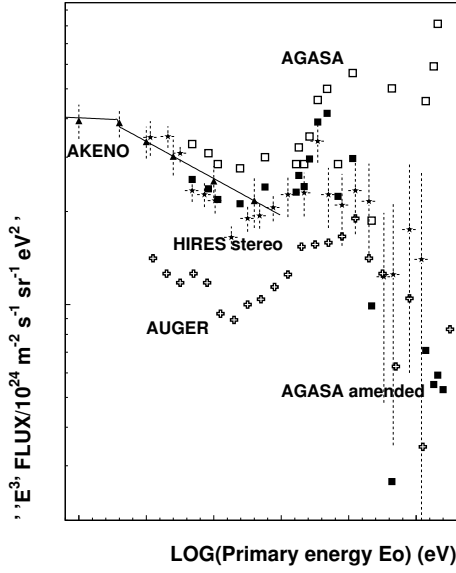


Fig. 4. Differential primary spectra for Akeno(full triangles), HiRes (stars), AUGER (crosses) [26], AGASA (open squares) as in [11] and a possible situation of AGASA data amended (full squares) after a specific treatment of inclined showers with Table I. The thin line is a fit to Akeno energy spectrum.

$$\left\{ \begin{array}{l} E_c = 10^{18.65} \text{ eV} \quad \gamma = 3.26 \quad A = 1.65110^{-32} \\ E_c = 10^{18.65} \text{ eV} \quad \gamma = 2.81 \quad A = 1.65110^{-32} \\ E_c = 10^{19.75} \text{ eV} \quad \gamma = 5.1 \quad A = 2.99210^{-37} \end{array} \right.$$

respectively for  $E_0 < 10^{18.65} \text{ eV}$ ,  $10^{18.65} \text{ eV} \leq E_0 \leq 10^{19.75} \text{ eV}$ ,  $E_0 > 10^{19.75} \text{ eV}$ . Another possible parameterization could be equation 4 for  $E_0 < 10^{18.65} \text{ eV}$  and for  $E_0 \geq 10^{18.65} \text{ eV}$ :

$$J(E_0) = A \times \left( \frac{E_0}{E_c} \right)^{-\gamma} \times \frac{1}{1 + \exp\left(\frac{\lg(E_0) - \lg(E_c)}{W_c}\right)} \quad (5)$$

where  $\gamma = 2.56$ ,  $E_c = 10^{19.75} \text{ eV}$ ,  $W_c = 0.16$  and  $A = 2.636 \cdot 10^{-32}$ . The last analytical representation was inspired by the astrophysical models assuming a uniform distribution of the sources with an injection spectral index of 2.2 combined with different energy cut off between  $10^{20}$  and  $10^{21} \text{ eV}$  [27]. The dip for the 3 spectra is close to  $10^{18.65} \text{ eV}$  ( $4.47 \cdot 10^{18} \text{ eV}$ ) corresponding to the  $e^+e^-$  production by a pure proton flux interacting in the extragalactic environment [28]. Herealso, AUGER measurements suggest a mixed primary component, instead the pure proton composition expected.

### III. SATELLITE EXPERIMENTS AND GIANT AIR SHOWERS

#### A. $\gamma$ Ray Astronomy from the sky

The discrimination by the maximum depth  $\langle X_{max} \rangle$  as it appears on Fig. 3 is considerably easier (LPM effect and limited consequences of the geomagnetic field in the pre-shower phase) between hadron and  $\gamma$ 's and may be the first

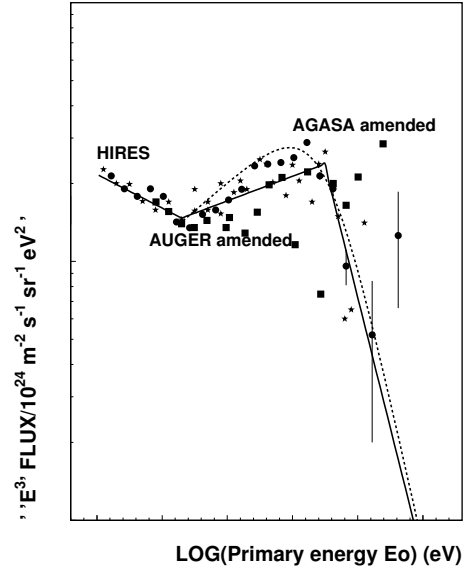


Fig. 5. An approach of the convergence to GZK : differential primary spectra for HiRes I, II (stars), AUGER (full circles)amended, AGASA (squares) amended

objective of satellite experiments, with the identification of the sources.

The case of geminated showers of ultra high energy could also be interesting taking the advantage of areas observed on about 1 million  $km^2$ . Pairs of  $\gamma$ 's as well as pairs  $\gamma$ -hadron may be observed as residues of GZK's type interaction in the interstellar medium or hadronic interactions in higher densities region in the galaxy. In this extent, a pair of  $\gamma$ 's of  $10 \text{ EeV}$  coming from  $\alpha$  Centaurus (4 l.y. distance) will be separated by about 700 km, when the same pair coming from the spiral arms of the galaxy will be lost.

The time delay  $\tau$  for one pair p- $\gamma$  or n- $\gamma$  varies as  $\frac{1}{\gamma_L^2}$  where  $\gamma_L$  is the Lorentz factor of the proton or the neutron. For a proton or neutron of  $100 \text{ EeV}$  from  $\alpha$  Centaurus, the delay  $\tau$  is around  $0.6 \mu\text{s}$  (respectively 1 ms for the spiral arms taken at 6000 l.y.).

#### B. The JEM-EUSO project

An analysis based on separation and time delay for pairs of cascades with an experiment like JEM-EUSO [30] would therefore be possible up to distances of 100 l.y. . With one pixel of the photoelectronic detector boarded on the ISS corresponding to  $1 \text{ km} \times 1 \text{ km}$  at ground level, the resolution on  $\langle X_{max} \rangle$  is better than  $50 \text{ gcm}^{-2}$  and the possibility of  $\gamma$  Ray Astronomy is obvious (Fig. 3 ); some improvements in the resolution will allow rapidly extension to measurements of mass composition and to energies lower than 50 EeV. According to the present data on Fig. 5 10000 events could be expected above GZK cutoff for an exposure of 5 years of JEM-EUSO (tilted mode with fluorescence scanning on

800000 km<sup>2</sup>. This statistics would fall approximately to 2500 events above 100 EeV and 150 events above 200 EeV.

#### IV. CONCLUSION

A tendency to the convergence between all the data of surface arrays supports the GZK behaviour. Some additive corrections in progress for AGASA, especially from the complex combination of the steepness of the spectrum data with the statistical fluctuations of the energy estimator will turn to a complete confirmation. The dependance of  $\langle X_{max} \rangle$  in AUGER above 30 EeV could be the indication of a change in p-air interaction such as an effect of phase transition to QGP and suppression of the leader [31] or an unexpected enhancement in heavy primaries at ultra high energy. Favourable circumstances appear to perform satellite detection of fluorescence, like in the JEM-EUSO project starting first with  $\gamma$  Ray Astronomy at ultra high energy.

#### ACKNOWLEDGEMENTS

The author would like to thank B. and S. Szabelski, as well as F. Cohen for their contribution to the original simulations and further interpretations

#### REFERENCES

- [1] D. Bergman, 30<sup>th</sup> ICRC, Merida, 1128 (2007).
- [2] A.V. Olinto, Proc. 28<sup>th</sup> ICRC, Tsukuba, 8, 299 (2003).
- [3] D. Bergman et al., HiRes Collaboration, Proc. 28<sup>th</sup> ICRC, Tsukuba, 1, 397-400 (2003).
- [4] J.N. Capdevielle, F. Cohen and K. Sanosyan, Proc. 28<sup>th</sup> ICRC, Tsukuba, 3, 1623 (2003).
- [5] D. Heck, J. Knapp, J.N. Capdevielle, G. Schatz and T. Thouw, FZK A report-6019 ed. FZK *The CORSIKA Air Shower Simulation Program*, Karlsruhe (1998).
- [6] J.N. Capdevielle and F. Cohen, J.Phys. G, Nucl. Part. Phys., 31, 507-524 (2005).
- [7] J. N. Capdevielle, C. Le Gall, K. Sanosyan, Astroparticle Physics, 13, 259 (2000).
- [8] M. Takeda et al., (AGASA collaboration), 28<sup>th</sup> ICRC, Tsukuba, 1, 381 (2003).
- [9] P. Sokolsky, P. Sommers and B. Dawson, Physics Reports, 217, 5, 253-277 (1992).
- [10] P. Sokolsky, inv. talk, XIV ISVHECRI, Weihai, (2006). Pune, 7, 59-62 (2005).
- [11] J.N. Capdevielle and F. Cohen, J.Phys.G 31, 1413-1419 (2005).
- [12] K. Shinozaki, inv. talk, XIV ISVHECRI, Weihai, (2006).
- [13] J.N. Capdevielle, F. Cohen, B. Szabelska, J. Szabelski, Proc. 20<sup>th</sup> ECRS, Lisbon (2006).
- [14] S. Yoshida et al., J. Phys. G 20, 651-664 (1994)
- [15] D. Bergman et al., 28<sup>th</sup> ICRC, Tsukuba, Rapporteur Volume, 299 (2003).
- [16] Aaron D. Chou, Phys. Rev. D, 74, 103001 (2006).
- [17] D. Heck, Vikhos CORSIKA School (2005)
- [18] R. Engel, Pierre Auger Collaboration, Proc. 30<sup>th</sup> ICRC, Merida 303 (2007)
- [19] D. Heck, Nucl. Phys. B, Proceedings supplement, 13<sup>th</sup> ISVHECRI, Pylos, 151, 127 (2006)
- [20] M. Unger, Pierre Auger Collaboration, Proc. 30<sup>th</sup> ICRC, Merida 594 (2007)
- [21] T. Pierog, Pierre Auger Collaboration, Proc. 30<sup>th</sup> ICRC, Merida 905 (2007)
- [22] M. Roth, Pierre Auger Collaboration, Proc. 30<sup>th</sup> ICRC, Merida 313 (2007)
- [23] F. Schmidt, Invited Contribution, 15th ISVHECRI, Paris (2008)
- [24] P. Sokolski, Nucl. Phys. B, Proceedings Supplement, 175-176, 207-212 (2008)
- [25] C. Meurer, Nucl. Phys. B, Proceedings Supplement, 175-176, 113-116 (2008)
- [26] T. Yamamoto, Pierre Auger Collaboration, Proc. 30<sup>th</sup> ICRC, Merida 318 (2007)
- [27] A.V. Olinto, D. Allard, E. Parizot, Astroparticle Physics, 27, 61-75 (2007)
- [28] V. Berezhinski et al., Phys. Rev. D, 74, 0403005 (2006)
- [29] J.N. Capdevielle, F. Cohen, B. Szabelska, J. Szabelski, submitted to J.Phys. G, (2008)
- [30] Y Takahashi, Nucl. Phys. B, Proceedings Supplement, 175-176, 237-240 (2008)
- [31] J.N. Capdevielle, F. Cohen and K. Sanosyan, Proc. 25<sup>th</sup> ICRC, Durban, 6, 293 (1997)